Research article

Received: 5 April 2018 Revised: 11 January 2019 Accepted: 15 January 2019 Published online in Wiley Online Library

(wileyonlinelibrary.com) DOI 10.1002/jib.560

Batch distillation of spirits: experimental study and simulation of the behaviour of volatile aroma compounds

Adrien Douady,[1] Cristian Puentes,[1] Pierre Awad[1,2] and Martine Esteban-Decloux[1]*

This paper focuses on the behaviour of volatile compounds during batch distillation of wine or low wine, in traditional Charentais copper stills, heated with a direct open flame at laboratory (600 L) and industrial (2500 L) scale. Sixty-nine volatile compounds plus ethanol were analysed during the low wine distillation in the 600 L alembic still. Forty-four were quantified and classified according to their concentration profile in the distillate over time and compared with previous studies. Based on the online recording of volume flow, density and temperature of the distillate with a Coriolis flowmeter, distillation was simulated with ProSim® BatchColumn software. Twenty-six volatile compounds were taken into account, using the coefficients of the 'Non-Random Two Liquids' model. The concentration profiles of 18 compounds were accurately represented, with slight differences in the maximum concentration for seven species together with a single compound that was poorly represented. The distribution of the volatile compounds in the four distillate fractions (heads, heart, seconds and tails) was well estimated by simulation. Finally, data from wine and low wine distillations in the large-scale alembic still (2500 L) were correctly simulated, suggesting that it was possible to adjust the simulation parameters with the Coriolis flowmeter recording and represent the concentration profiles of most of the quantifiable volatile compounds. © 2019 The Institute of Brewing & Distilling

Keywords: batch distillation; copper still; spirits; volatile aroma compounds; simulation

Introduction

The diversity of distilled spirits consumed around the world is large. In Europe, the definition, description, labelling and protection of geographical indications of spirit drinks are specified in regulation 110/2008 *(1)*. The standard unit for ethanol concentration is the alcoholic strength by volume (annex I point 11), or ABV (alcohol by volume) in % v/v. The distillation process concentrates the ethanol and volatile aroma compounds from the fermented must, as well as those formed *in situ* through chemical reactions *(2)*. The quality and specific characteristics of a spirit beverage are highly dependent on the nature and concentration of the volatile compounds and, to a lesser extent, its ethanol concentration. The volatile compounds responsible for the overall aroma perception of spirit beverages belong to many chemical families, such as alcohols, carboxylic acids, esters and aldehydes *(2)*. The precise relationship between volatile compounds and aroma perception is still difficult to assess, owing to the variable nature of volatile compounds, concentration relative to sensory threshold and possible synergies. The diversity of volatile compounds and differences in concentration is mainly due to the raw materials, fermentation method and the distillation process, which includes both the apparatus and the method *(3,4)*.

Three main methods are commonly used with a typical distillation apparatus: (a) continuous distillation in a multistage distillation column (e.g. rum, vodka, Armagnac, Calvados, neutral alcohol), (b) batch (simple discontinuous) distillation involving recycling (e.g. Cognac, Armagnac, Auge, Calvados, rum) and (c) batch distillation in a column involving recycling (fruit brandies). The preferred method depends on the organoleptic qualities desired. For instance, full-bodied, single malt whiskies are produced with a batch method in traditional pot stills, while lighter grain whiskies are produced in multistage distillation columns *(5)*. According to Ferrari *et al*. *(6)*, the behaviour of volatile compounds is different during distillation in pot stills and rectification columns. Indeed, in contrast to esters, it was observed that larger quantities of higher alcohols were recovered in the distillate in continuous distillation than in the simple batch process.

This study focused on the behaviour of volatile compounds during simple batch distillation. This method is generally conducted in a traditional copper still, known as an 'alambic charentais' (Fig. 1) *(3,7–9)*. Distillation is carried out in two successive cycles. During the first cycle, known as 'wine distillation', the wine is introduced into the boiler. An initial small fraction of distillate ('heads') is collected and separated. Distillation then continues until the ABV of the distillate reaches ~2% v/v. This second fraction constitutes the low wine, with ethanol concentration between 27 and 30% v/v. The second cycle is the low wine distillation. In analogy with wine distillation, the first fraction of distillate ('heads') with the highest ethanol concentration is removed. The 'heart' is collected and separated once the ethanol concentration of the distillate

* Correspondence to: Martine Esteban-Decloux, AgroParisTech. 1 av des Olympiades 91300 Massy, France. E-mail: martine.decloux@agroparistech.fr

[1] Unité Mixte de Recherche Ingénierie Procédés Aliments, AgroParisTech, INRA, Université Paris-Saclay, F-91300, Massy, France

[2] Unité Mixte de Recherche Génie et Microbiologie des Procédés Alimentaires, AgroParisTech, INRA, Université Paris-Saclay, 78850, Thiverval-Grignon, France

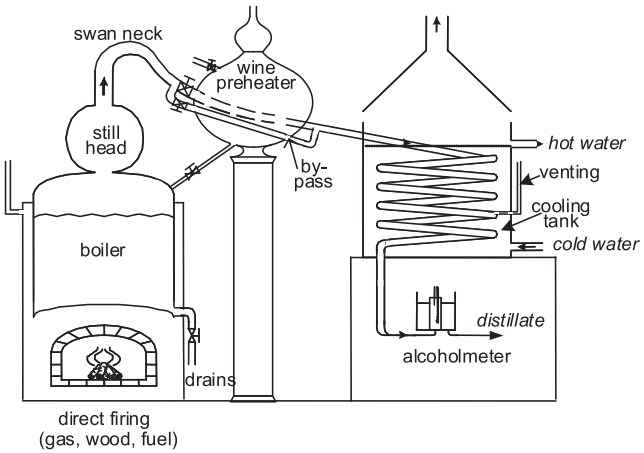

Figure 1. Diagram of a traditional Charentais copper still.

reaches ~60% v/v. The average ethanol concentration of the heart must be <72.4% v/v for Cognac *(10)*. The last two fractions are the 'seconds' and 'tails'. The heart constitutes the spirit (or *eau-de-vie*) and is placed in an oak barrel for aging. All the other distillate fractions are recycled back into the process. Several methods exist but heads and tails are usually recycled in the wine and seconds in the low wine. After the tails, when the gas burner is turned off, a small fraction of distillate, known as '*petites-eaux*', is sent directly to the distillation residue storage.

Despite its long history, batch distillation is still poorly understood. In order to acquire knowledge about the behaviour of volatile compounds, the National Interprofessional Committee of Cognac conducted experimental investigations in 1989. Both distillations (wine and low wine) were sampled in an operational plant. Fifty-seven volatile compounds were analysed and 39 concentration profiles in the distillate were drawn as a function of decreasing ABV and classified in different types *(7)*, as shown in Fig. 2 and Table 1. Types 1, 2, 3 and 6 were present in both wine and low wine distillations, while types 4 and 5 were specific to the wine distillation and types 7 and 8 to the low wine distillation. Types 1, 7 and 8 were representative of highly volatile compounds that concentrate in the first running of distillate. Types 3 and 4 were present in all fractions of distillate. Types 2, 5 and 6 corresponded to low volatile compounds, which increased in concentration with decreasing alcohol strength. Unfortunately, neither the composition

Table 1. Classification volatile compounds during batch distillation by Cantagrel *(7)*

Type	Classification of compounds during wine distillation
1	Acetaldehyde, 1,1-diethoxy-ethane, 1,1-diethoxy-methyl-2-propane, ethyl acetate, ethyl propanoate, ethyl butanoate, ethyl caproate, ethyl caprylate, ethyl caprate, ethyl laurate, ethyl myristate, ethyl palmitate, ethyl stearate, ethyl oleate, ethyl linoleate, ethyl linolenate, isoamyl acetate, isoamyl caprate
2	Furfural
3	Methanol
4	1-Propanol, 2-methyl-1-propanol, 1-butanol, 2-methyl-1-butanol, 3-methyl-1-butanol, 2-phenylethyl acetate
5	2-Phenylethanol
6	Ethyl lactate, diethyl succinate
	Classification of compounds during low wine distillation
1	Acetaldehyde, 1,1-diethoxy-ethane, 1,1-diethoxy-methyl-2-propane, ethyl acetate, ethyl propanoate, ethyl butanoate, hexyl acetate, ethyl caproate, ethyl laurate, ethyl myristate, ethyl palmitate, isobutyl caprate, isoamyl acetate, isoamyl caprylate, isoamyl caprate, isoamyle myristate
2	2-Phenylethanol
3	Methanol
6	Furfural, 2-phenylethyl acetate, ethyl lactate, diethyl succinate, caprylic acid, capric acid, lauric acid
7	1-Propanol, 2-methyl-1-propanol, 1-butanol, 2-methyl-1-butanol, 3-methyl-1-butanol, ethyl stearate, ethyl oleate, ethyl linoleate, ethyl linolenate
8	Ethyl caprylate, ethyl caprate.

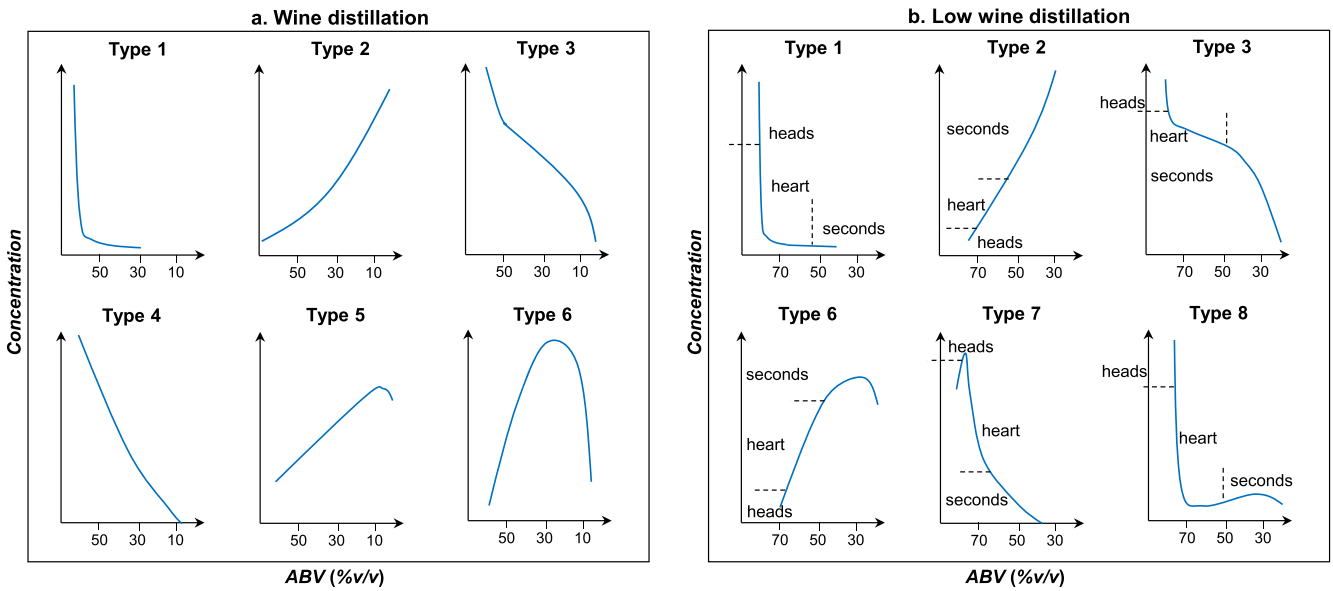

Figure 2. Concentration profiles of volatile compounds during distillation. Adapted from *(7,8)*. [Colour figure can be viewed at wileyonlinelibrary.com]

of the liquids introduced into the boiler (ABV, volatile compound concentrations), the distillation parameters (heating power profile, volumes, cut criteria) nor the concentrations of the volatile compounds in the distillates were reported in this study. More recently, Lukić *et al. (11)* investigated the distribution of 155 volatile compounds among the various cuts (heads, heart 1 to heart 3, and tails) during the distillation of fermented Muscat wines, in a traditional 120 L alembic still, heated over a direct open flame. They highlighted the importance of distillation cut criteria on the heart composition and the recycling of the tails fraction in the next distillation, in order to enrich the liquid to be distilled in the monoterpenes and C_{13} norisoprenoids responsible for varietal aromas. Spaho *et al. (12)* investigated the impact of the ethanol concentration of the cut between the heart and tails on the distribution of higher alcohols and esters, as well as the organoleptic characteristics of the heart fraction of fruit brandy made from three plum varieties, using a traditional 10 L copper still heated over a direct flame. Silva *et al. (13)* studied the impact of repeated batch distillations of mono-distilled organic sugarcane spirit, using a 12 L copper still, to improve product quality to meet national and international standards. Balcerek *et al. (14)* studied the influence on plum brandy of the batch distillation method (initial distillation in a 35 L copper still heated with a water steam jacket, followed by a second distillation in a column or a single distillation in a column) and the ethanol concentration of the heart on its volatile composition, organoleptic characteristics and concentrations of volatile compounds harmful to human health (e.g. methanol, hydrocyanic acid and ethyl carbamate). Awad *et al. (9)* characterised the volatile compounds produced by chemical reactions during the batch distillation of Cognac in an industrial scale alembic (2500 L), using real wines and low wine. Sampling and analysis of the initial wine and low wine and the distillate fractions and residues, as well as volume measurements, provided data for mass balances. They identified several types of volatile compounds that increased significantly in quantity during distillation. It was found that the wine distillation was key to the formation of volatile compounds.

In parallel to this experimental approach, many researchers have used simulation to explore the behaviour of the volatile compounds and the influence of the operating parameters on distillation. Many studies have been published on continuous distillation in multistage columns *(5,15–19)*, batch distillation in columns *(20,21)* or alembic *(22,23)*. For batch distillation in alembic stills, Scanavini *et al. (22)* and Sacher *et al. (23)* developed models that need computational modification to be adapted to other distillation units. Scanavini *et al. (22)* compared simulated data with two experimental distillations with a synthetic solution of seven volatile compounds, conducted in a laboratory scale (8 L) still, heated over a direct open flame. Good agreement between experimental and simulated data was observed for the ethanol concentration profile, temperature in the boiler and volatile compounds in the heart. The model developed by Sacher *et al. (23)* was calibrated using a laboratory scale (2 L) copper heated by an electric resistor and with 17.9% v/v pear distillate. They compared their results with the quantification of 15 volatile compounds. Good correlation was observed between experimental and simulated data for each fraction of distillate (heads, heart, seconds, tails). The concentration profiles over time for most volatile compounds were in agreement with those published by Cantagrel *(7)*. The only exception was 2-phenylethanol, as the model used to estimate the vapour–liquid equilibrium data [UNIFAC Dortmund 1993, a predictive method developed by *(24)* for the estimation of thermodynamic properties] was not adapted to this type of compound in hydro-alcoholic solution. In fact, when data predicted by this UNIFAC model were compared with experimental findings of Athès *et al. (25)*, the predicted volatility was overestimated and, consequently, the predicted concentration in the heart.

A good knowledge of liquid–vapour equilibria is indispensable to simulate a distillation process *(18,26)*. Puentes *et al. (26)* carried out a bibliographic review, gathering all available data on liquid–vapour equilibria for volatile compounds in hydro-alcoholic solutions, covering 44 volatile compounds belonging to several chemical families (12 alcohols, 12 esters, nine carboxylic acids, one acetal, seven carbonyl compounds, one furan and two terpenes). The 'Non Random Two Liquids' (NRTL) model was selected to represent the non-ideality of the solution *(27)*, as advised by Batista and Meirelles *(15)* and Valderrama *et al. (17)*. For modelling purposes, the interactions between the volatile compounds and the solvent (ethanol–water) were taken into account, whereas those between volatile compounds were ignored, owing to their low concentrations. These data were used to classify the volatile compounds into three main groups, according to their relative volatilities with respect to ethanol and water, over the entire range of ethanol concentrations: (a) light (more volatile than ethanol); (b) intermediate (less volatile than ethanol, but more volatile than water); and (c) heavy (less volatile than water).

In this context, the present work focused on the behaviour of volatile compounds during a batch distillation in alembic stills with real wine or low wine in traditional copper Charentais stills, heated over a direct open flame, on laboratory (600 L) and industrial (2500 L) scales. BatchColumn software (ProSim®) configured with the set of interaction parameters determined by Puentes *et al. (26)* was used to assess the potential of commercial software to represent experimental distillation data.

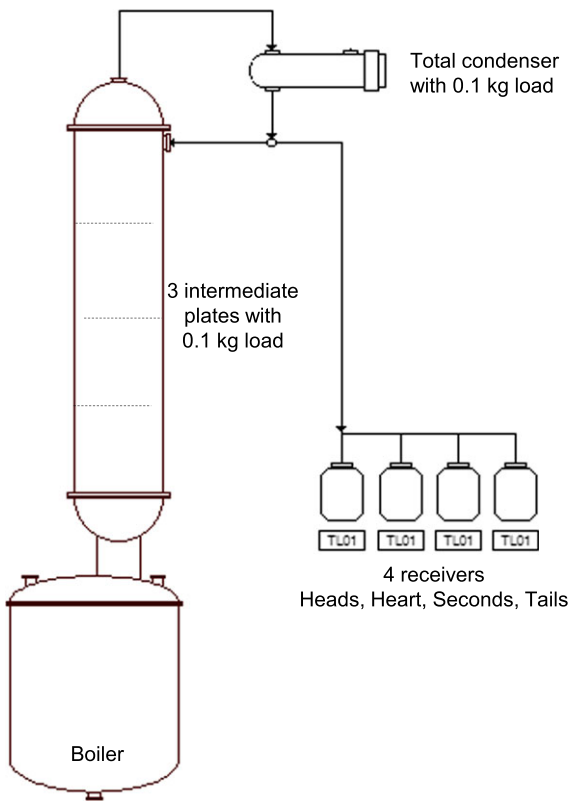

Figure 3. Diagram of the batch distillation unit simulated in the BatchColumn software. [Colour figure can be viewed at wileyonlinelibrary.com]

Material and methods

Distillation

One experiment was conducted with a 600 L copper still, heated over a direct open flame, composed of a boiler, a wine heater and a cooler (Figure 1). The installation included several temperature probes (PT 100 sensors), a Coriolis flowmeter (Emerson, micro motion® F-Serie 050) and a data recording using InTouch 2014 R2 software, developed by Wonderware®. The Coriolis flowmeter, between the alcoholmeter receiver and the storage tanks, provided continuous measurement of distillate density, volume flow and temperature. Online data were recorded every minute, except for volume flow, where the values recorded were the average over the previous 60 s. The low wine was introduced into the boiler. Heating power was fixed by gas pressure: 815 mbar to reach boiling point, 115 mbar during production of the heads, and then 195 mbar for the heart, seconds, and tails. Distillation cuts were determined by the ethanol concentration, indicated by the alcoholmeter and recorded. Four fractions of distillate were collected: heads, heart, seconds and tails. The heads did not pass through the Coriolis flowmeter, to avoid clogging, so no data was recorded. The volume and temperature of each fraction were measured. The volume of the residue was deduced from the material balance, as detailed below. At the end of the distillation, when the gas was turned off, the *petites-eaux* fraction passed directly into the main tank and was not collected.

Experimental data obtained in a previous study by Awad *et al.* *(9)* were used to assess the potential of the simulation software to represent the experimental data obtained using a standard size copper still (2500 L), the maximum capacity authorised for Cognac distillation *(10)*. Supplementary data measured (but not published) by these authors (gas pressure, distillate strength and flow rate) were also used here for comparison purposes. The density, temperature and volume flow of the distillate were measured by a Coriolis flowmeter (Endress Hauser® LPG). These values, together with gas pressure, were recorded every 10 s.

Table 2. Offline mass balance ethanol–water

	Products	$x_{m\text{-}eth}$	m (kg)	M_{eth} (kg)
In	Low wine (LW)	0.2574	584.75	150.53
Out	Heads (H)	0.7025	3.48	2.45
	Heart (Ht)	0.6481	181.07	117.36
	Seconds (S)	0.3143	92.40	29.04
	Tails (T)	0.0681	20.73	1.41
	Petites-eaux (PE)	0.2557	4.47	0.11
	$D = \sum$ distillate	0.4977	302.15	150.37
	Residue (R)	0.0005	282.60	0.15
	$D + R$		584.75	150.52
	Mass balance: LW − ($D + R$)		0.0	0.01

Table 3. Comparison between offline and online data ethanol measurements

Initial sampling time (min)	Final sampling time (min)	$x_{m\text{-}offline}$ sample measurement	$x_{m\text{-}online}$ average of three values	Difference (%)
154	157	0.7086	0.7092	0.08
214	217	0.6915	0.6923	0.12
274	277	0.6652	0.6675	0.34
334	337	0.6339	0.6341	0.04
394	397	0.5863	0.5868	0.09
490	493	0.4709	0.4737	0.59
550	554	0.3708	0.3720	0.32
610	614	0.2642	0.2616	0.99
670	674	0.1525	0.1603	5.12

Sampling

In the first experiment – distillation in a 600 L copper still – the low wine was introduced into the boiler and each fraction (heads, heart, seconds and tails) together with the residue were sampled to quantify the volatile compounds. To obtain information about the behaviour of the volatile compounds, distillate samples (1.4 L) were taken from the heart (five samples) and seconds (four samples) after 30 min and then every hour. In total, 15 samples were collected.

Determining ethanol concentration and ethanol–water mass balances

Samples from low wine distillation in the 600 L copper still were analysed by the Union Nationale du Groupement des Distilleries Agricoles (UNGDA) laboratory (Malakoff, France). The ethanol concentration (ABV) of the samples (low wine, distillates and residue) was determined from density measurement at 20°C, using an Anton Paar® DMA 500 densitometer. These solutions were considered as a binary hydro-alcoholic system, being composed of water, ethanol and highly dilute volatile compounds. The error generated by this assumption on the ABV estimation varied between 0.5 and 1% *(28)*. Ethanol mass concentrations ($X_{m\text{-}eth}$, g of ethanol/g of solution) were derived from these data.

The volume, temperature and ethanol concentration of each fraction of distillate (heads, heart, seconds and tails) were measured in the tanks. To estimate the mass of each fraction, it was necessary to compute the density of the solution at the measured temperature. An Excel macro edited with Visual Basic was developed, using the equation from the International Alcoholometric Tables *(29)*.

Table 4. Mass balances – comparison between offline and online data

	x_m ($g_{ethanol}/g_{solution}$)			m (kg)			M_{eth} (kg)		
Product	Offline	Online	Difference (%)	Offline	Online	Difference (%)	Offline	Online	Difference (%)
Heart (Ht)	0.648	0.645	0.46	181.07	173.26	4.51	117.36	112.24	4.56
Seconds (S)	0.314	0.320	1.87	92.40	90.37	2.25	29.04	28.91	0.45
Tails (T)	0.068	0.073	6.85	20.73	20.35	1.87	1.41	1.49	5.40

One of the goals of this study was to assess the potential of the simulation tool to represent experimental data. To do this, it was first necessary to check the consistency of the experimental data, both offline (from the sample and tank measurements) and online (from the Coriolis flowmeter recordings). The offline data was evaluated by an ethanol–water mass balance and then compared with the on-line mass balances. As the *petites-eaux* fraction was neither collected nor taken into account in the residue sample, its ethanol concentration was deduced from the last drops of tails and the residue.

For each fraction (j), the total mass of distillate (m_j, kg solution) and the mass of ethanol ($m_{eth\text{-}j}$, kg ethanol) were determined using the volume (V, L solution), density (ρ, kg/L solution) and ethanol mass concentration ($X_{m\text{-}eth}$, g ethanol/g solution) in the various tanks, plus the samples analysed at the UNGDA, according to equations (1) and (2).

$$m_j = V_{tank-j} \times \rho_{tank-j} + \sum_{k=1}^{\text{nb of samples}} V_k \times \rho_k \quad (1)$$

$$m_{eth-j} = V_{tank-j} \times \rho_{tank-j} \times X_{m-eth-tank-j} + \sum_{k=1}^{\text{nb of samples}} V_k \times \rho_k \times X_{m-eth-k} \quad (2)$$

Then for each fraction (heart, seconds and tails), according to equations (3) and (4), ethanol–water mass balances were determined from online recorded data [volume flow (FT, L/h solution), density (ρ, kg/L solution), temperature (T, °C) and time] and calculated ethanol concentration (X_{m_eth}, g ethanol/g solution) from density and temperature, as explained previously.

$$m_j = \sum_{k=1}^{\text{length of time (min)}} FT_k/60 \times \rho_k \quad (3)$$

$$m_{eth-j} = \sum_{k=1}^{\text{length of time (min)}} FT_k/60 \times \rho_k \times X_{m-eth-k} \quad (4)$$

Volatile compound analysis and mass balances

Volatile compounds were analysed by the UNGDA using the methods reported in Puentes *et al.* *(28)*. Sixty-nine volatile

Table 6. Classification of experimental data and comparison with Cantagrel *(7)*

Type 1	**Type 2**	**Type 7**
Acetaldehyde[a]	Formic acid[c]	1-Propanol[a]
1,1-Diethoxy-ethane[a]	Acetic acid[c]	2-Methyl-1-propanol[a]
Ethyl acetate[a]	Lactic acid[c]	2-Methyl-1-butanol[a]
Ethyl butanoate[a]	**Type 3**	3-Methyl-1-butanol[a]
Ethyl caproate[a]	Methanol[a]	1-Hexanol[c]
Ethyl laurate[a]		(*Z*)-3-Hexenol[c]
Ethyl myristate[a]	**Type 6**	1-Tetradecanol[c]
Ethyl palmitate[a]	Caprylic acid[a]	(*E*)-Nerolidol[c]
Isoamyl acetate[a]	Capric acid[a]	α-Terpineol[c]
Isoamyl caprylate[a]	Lauric acid[a]	
Hexyl acetate[a]	Ethyl lactate[a]	**Not well represented**
Ethyl caprylate[b]	Furfural[a]	Linalool[c]
Ethyl caprate[b]	Diethyl succinate[a]	Myristic acid[c]
Ethyl stearate[b]	2-Phenylethanol[b]	Palmitic acid[c]
Ethyl oleate[b]	Isobutanoic acid[c]	2-Phenylethyl caprylate[c]
Ethyl linoleate[b]	2-Methylbutanoic acid[c]	
Isoamyl laurate[c]	Isovaleric acid[c]	
	Caproic acid[c]	

[a]Similar;
[b]different;
[c]not analysed by Cantagrel *(7)*.

Table 5. Volatile compound mass balances (Out/In)

	Out/In		Out/In		Out/In
Methanol[a]	0.98	Ethyl acetate[a]	1.07	Linalool	0.69
1-Propanol[a]	0.97	Ethyl lactate [a]	0.97	α-Terpineol	0.87
2-Methyl-1-propanol[a]	0.99	Ethyl caproate [a]	1.09	(*E*)-Nerolidol	1.53
2-Methyl-1-butanol[a]	1.02	Ethyl caprylate[a]	1.14		
3-Methyl-1-butanol[a]	1.02	Ethyl caprate [a]	1.30	Formic acid	1.30
1-Hexanol	1.07	Ethyl laurate [a]	1.50	Acetic acid	0.74
(*Z*)-3-Hexenol	1.24	Isoamyl acetate[a]	1.09	Isobutanoic acid	0.78
2-Phenylethanol[a]	0.60	Ethyl butanoate[a]	1.19	2-Methylbutanoic acid	0.84
1-Tetradecanol	1.20	Hexyl acetate[a]	1.12	Isovaleric acid	0.88
		Isoamyl caprylate[a]	1.37	Lactic acid	3.36
Acetaldehyde[a]	0.80	2-Phenylethyl caprylate	0.70	Caproic acid	0.80
		Diethyl succinate[a]	0.87	Caprylic acid[a]	0.81
Furfural[a]	0.96	Isoamyl laurate	2.45	Capric acid[a]	0.83
		Ethyl myristate[a]	1.86	Lauric acid[a]	0.98
1,1-Diethoxy-ethane [a]	0.78	Ethyl palmitate[a]	2.19	Myristic acid	0.92
		Ethyl stearate[a]	2.25	Palmitic acid	0.87
		Ethyl oleate[a]	1.91		
		Ethyl linoleate[a]	2.27		

[a]Volatile compounds analysed by Cantagrel *(7)*.

compounds were quantified (16 alcohols, 20 esters, 19 carboxylic six terpenes, two lactones, two furans, two acetals, one carbonyl compound and one norisoprenoid). Owing to the large range of ethanol concentrations among the samples, they were classified in two groups: (a) in samples of low wine, heads, heart and seconds, the ABV was adjusted to 40% v/v and (b) in samples from the tails and residue, the ABV was adjusted to 12%. This standardisation of the ethanol concentration with deionised water or anhydrous alcohol reduced the matrix effects on the quantification of volatile compounds. Considering the variety of volatile compounds to be analysed (chemical family and concentration), three different methods were implemented. For volatile compounds present at high concentrations, direct injection into the gas chromatograph was effective. However, for volatile compounds at low concentrations (0.1–0.9 mg/L), liquid–liquid extraction using organic solvent was necessary before injection. Finally, for compounds with very low volatility, such as carboxylic acids, for which gas chromatography is not an appropriate technique, a pre-treatment step of derivatisation was required to convert them into benzylic esters.

In the same way, the offline data was assessed by way of a mass balance for each volatile compound analysed. For each fraction *j*, the mass fraction of each volatile compound *i* ($X_{m\text{-}i/j}$) was calculated with equation (5), using the concentration (mg/L) determined by the UNGDA laboratory and the calculated density of the solution (kg/L).

$$X_{m-i/j}\left(\frac{g}{g}\right) = \frac{\text{concentration}}{\text{density}} \times 10^{-6} \tag{5}$$

Then, the mass of volatile compounds *i* in fraction *j* was deduced from mass fraction ($X_{m\text{-}i/j}$) and the total mass of the fraction (m_j). As previously, for fractions where several samples were collected during distillation (heart and seconds), the mass of volatile compounds *i* in fraction *j* was calculated with equation (6).

$$m_{i/j} = X_{m-i/\text{tank}-j} \times m_{\text{tank}-j} + \sum_{k=1}^{\text{nb of samples}} X_{m-i/k} \times m_k \tag{6}$$

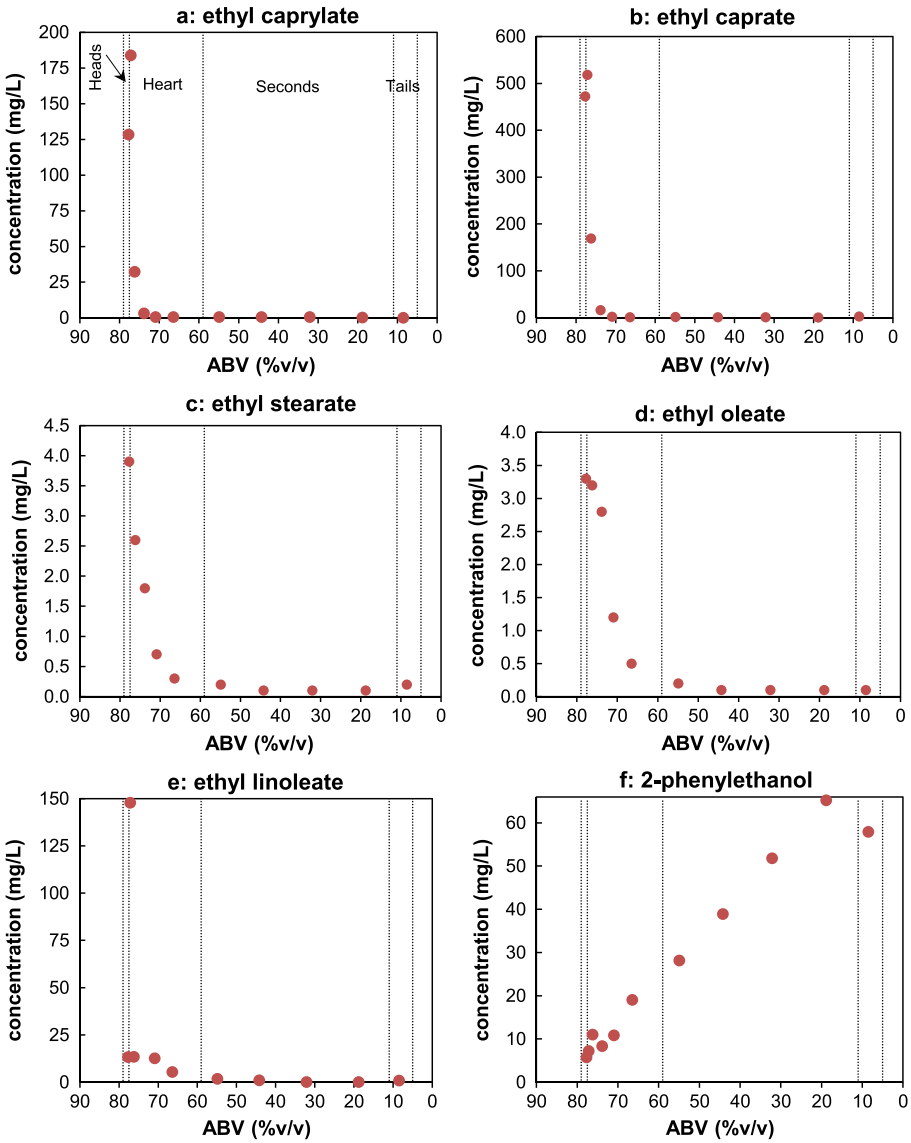

Figure 4. Volatile compounds with concentration profiles different of Cantagrel *(7)*. [Colour figure can be viewed at wileyonlinelibrary.com]

Creation of the simulation tool with ProSim BatchColumn software

BatchColumn software (ProSim®) was used to simulate the experimental distillation unit. This simulation tool includes a rigorous dynamic model for the design and analysis of batch distillation processes. Among the volatile compounds quantified, 36 were present in the ProSim Simulis database. Regarding the thermodynamic modelling, the vapour phase was represented with the ideal gas law. In the case of carboxylic acids, capable of forming dimers owing to strong hydrogen bonds, this was combined with an association model *(30)*. The non-ideality of the liquid phase was represented with the NRTL model, using the interaction parameters estimated by Puentes *et al. (26)*. The interaction parameters for four supplementary alcohols (1-octanol, 1-decanol, 1-dodecanol and 1-tetradecanol) were derived from the predictions of the UNIFAC Dortmund model (1993).

The simulation module (Fig. 3) was designed with five trays (cooler, three intermediate trays and the boiler) to take into account the internal reflux owing to heat losses through the still-

Table 7. Comparison with the classification by Puentes *et al. (28)*

Light		Intermediate		Heavy
Type 1	**Type 7**	**Type 3**	**Type 6**	**Type 2**
Acetaldehyde	1-Propanol	Methanol	Caprylic acid	Formic acid
Ethyl acetate	2-Methyl-1-propanol		Ethyl lactate	Acetic acid
Ethyl butanoate	2-Methyl-1-butanol		2-Phenylethanol	
Ethyl caproate	3-Methyl-1-butanol		Isobutanoic acid	
Isoamyl acetate	1-Hexanol		Isovaleric acid	
Hexyl acetate	(*Z*)-3-Hexenol		Caproic acid	
Ethyl caprylate	1-Tetradecanol			
Ethyl caprate				

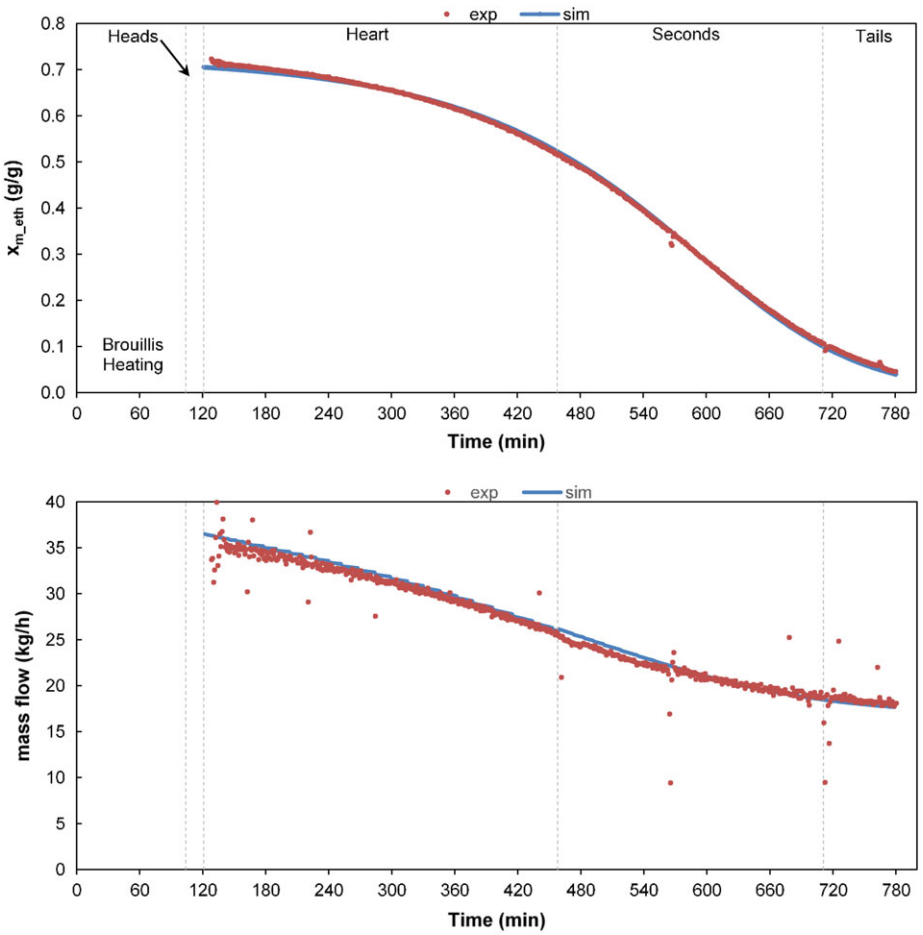

Figure 5. Experimental and simulated profiles during low wine distillation (600 L). [Colour figure can be viewed at wileyonlinelibrary.com]

head. Nevertheless, to minimise the exchange through the three intermediate trays, very small loads of liquid were considered (0.1 kg each). An efficiency of 0.9 was established for the boiler and 0.63 for the intermediate trays. These values were chosen *a priori* to represent the mass flow and ABV concentration of the distillate over time. The pressure of the installation was set at the standard atmosphere without pressure loss. Four tanks were connected to the cooler output to collect the distillate fractions (heads, heart, seconds and tails).

The initial mass, composition and temperature of the load in the boiler were taken from experimental data. The simulation was developed in five steps: heating the low wine to boiling point, followed by the separation of the distillate into four fractions (heads, heart, seconds and tails). The duration of each step was equivalent to the corresponding experimental value. During the distillation process, two adjustable parameters were the heating power (*Qb*) and internal reflux level (*R*). For the first step, heating power was estimated using the mass of liquid introduced into the boiler, its specific heat (dependent on ethanol concentration), the temperature difference between the initial value and boiling point (also dependent on ethanol concentration) and the duration of this step. Then heating power and reflux ratio were adjusted to obtain good agreement with the experimental mass flow and ethanol concentrations over time.

Results and discussion

For the experiment with the 600 L alembic still, a global ethanol–water mass balance was calculated using the experimental offline data, and its consistency was evaluated. Then, for each distillate fraction (except the heads), the mass and ethanol concentration in the online data were compared with offline data to verify their coherence. The mass balance was calculated for each volatile compound *i* and its concentration profile during distillation was compared with data reported by Cantagrel *(7)*. Simulated data (mass flow, ABV, concentration profiles and distributions of volatile compounds) were compared with experimental data. Finally, the experimental distribution of volatile compounds obtained during the distillation of wine and low wine in the 2500 L alembic still were compared with the simulated results.

Global and ethanol mass balances

Ethanol concentration and the volume and temperature of each distillate fraction were used to calculate the total and ethanol–water mass balances (Table 2). The ethanol concentration of the *petites-eaux* fraction, which was not collected, was calculated from the last ethanol concentration measured in the tails (5.9% v/v), the average ethanol concentration of the residue (0.07% v/v) and the volatility of ethanol at this concentration. The ethanol concentration was 3.33% v/v, corresponding to a 0.026 (g/g) ethanol mass fraction. To obtain a coherent balance, the volume of low wine had to be increased from 600 to 609 L, a variation within the precision range of the volume introduced into the boiler.

The ethanol concentration measured in samples collected during distillation (heart and seconds) were compared with average values from online data. The small differences obtained (Table 3) suggest that the ethanol concentration estimated from the Coriolis

Table 8. Comparison between experimental and simulated concentration profiles

Overlaid curves (18 species)		Curves with the same shape but differences in maximum concentration (7)	Inconsistent curves (1)
Methanol	Ethyl caprylate	2-methyl-1-butanol	Formic acid
1-Propanol	Ethyl caprate	1-Hexanol	
2-Methyl-1-propanol	Isoamyl acetate	Furfural	
3-Methyl-1-butanol	Ethyl butanoate	Ethyl lactate	
(*Z*)-3-Hexenol	Hexyl acetate	Isobutanoic acid	
2-Phenylethanol	Acetaldehyde	Caproic acid	
1-Tetradecanol	1,1-Diethoxy-ethane	Caprylic acid	
Ethyl acetate	Acetic acid		
Ethyl caproate	Isovaleric acid		

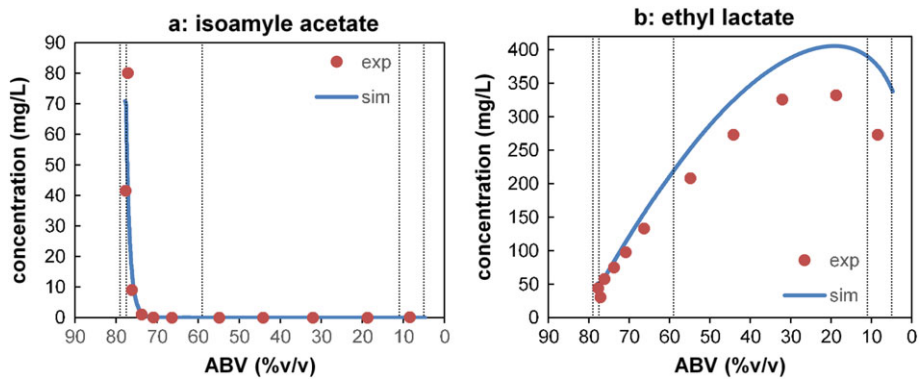

Figure 6. Experimental and simulated concentration profiles for two esters. [Colour figure can be viewed at wileyonlinelibrary.com]

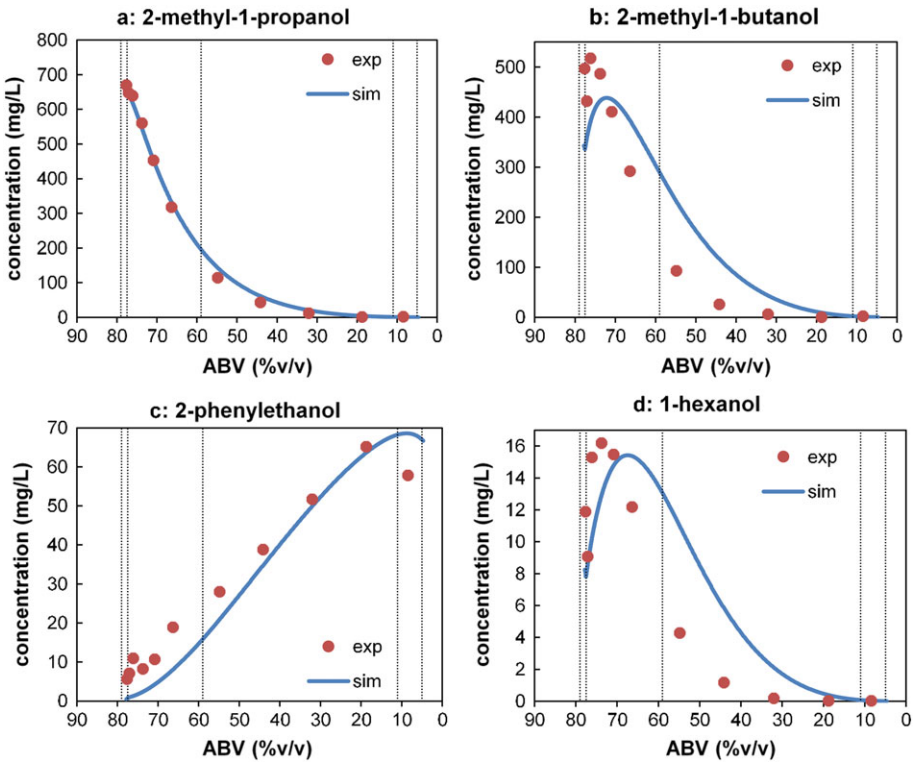

Figure 7. Experimental and simulated concentration profiles for four alcohols. [Colour figure can be viewed at wileyonlinelibrary.com]

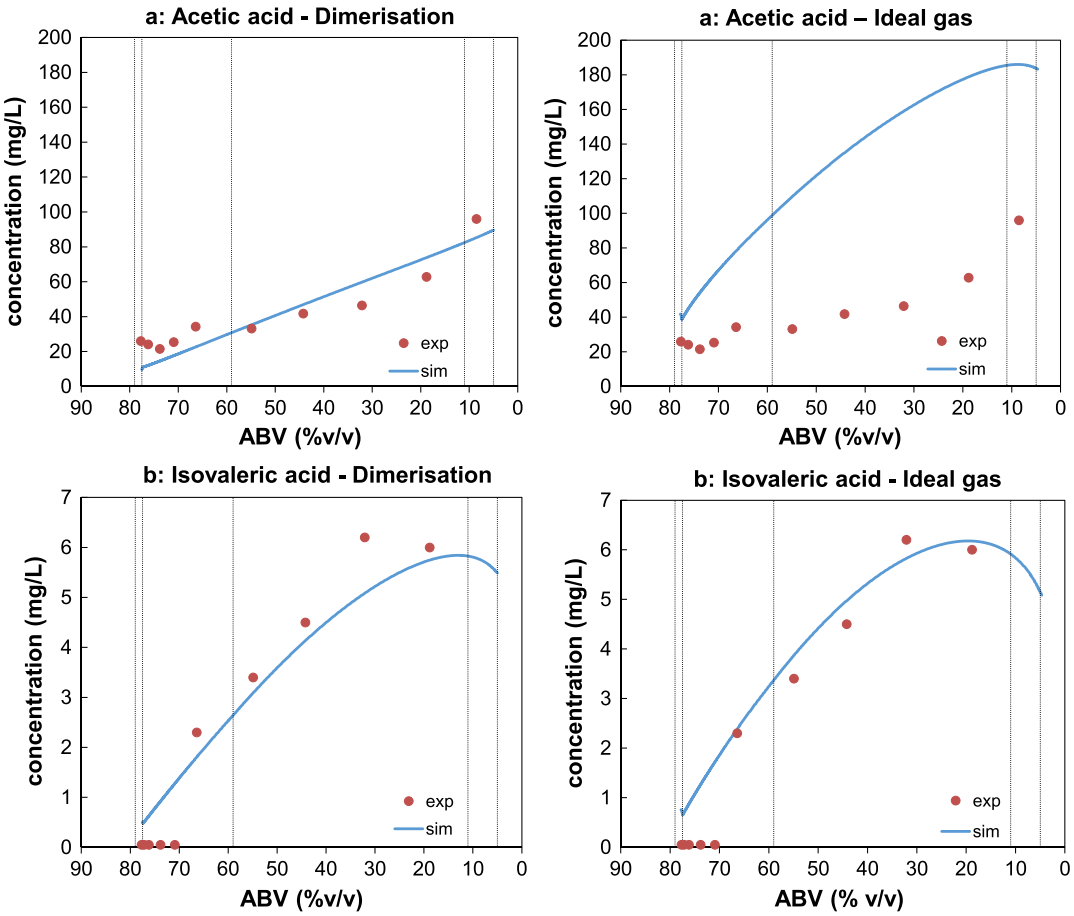

Figure 8. Experimental and simulated concentration profiles for two acids with and without dimerisation. [Colour figure can be viewed at wileyonlinelibrary.com]

Table 9. Distribution of volatile compounds during low wine distillation in a 600 L copper still

Compound	CAS	Heads (%)		Heart (%)		Seconds (%)		Tails (%)		Residue (%)		Heart + seconds (%)	
		Experimental	Simulated	Experimental	Simulated	Experimental	Simulated	Experimental	Simulated	Experimental	Simulated	Experimental	Simulated
Ethanol	64–17-5	1.62	1.64	77.97	77.92	19.29	19.15	0.94	0.86	0.17	0.44	97.27	97.07
Methanol	67–561	1.6	1.3	66.0	65.1	24.9	26.8	2.5	3.1	5.0	3.7	90.9	92.0
1-Propanol	71–23-8	1.7	1.7	80.4	83.0	13.8	15.0	0.3	0.3	3.8	0.1	94.2	98.0
2-Methyl-1-propanol	78–83-1	2.3	2.3	92.1	92.2	4.2	5.5	0.1	0.0	1.3	0.0	96.4	97.7
2-Methyl-1-butanol	137–32-6	1.9	1.4	92.6	87.2	3.9	11.3	0.1	0.0	1.5	0.0	96.5	98.6
3-Methyl-1-butanol	123–51-3	1.6	1.7	92.1	90.1	5.9	8.2	0.1	0.0	0.4	0.0	98.0	98.3
1-Hexanol	111–27-3	1.2	1.0	92.8	82.5	5.0	16.5	0.1	0.0	0.9	0.0	97.8	99.0
(*Z*)-3-Hexenol	928–96-1	0.9	1.1	73.0	81.1	19.4	17.6	0.5	0.1	6.3	0.0	92.4	98.8
2-Phenylethanol	60–12-8	0.2	0.0	18.2	6.6	37.6	34.0	10.4	12.2	33.7	47.1	55.7	40.6
1-Tetradecanol	112–72-1	5.7	0.9	84.3	98.3	6.6	0.8	1.4	0.0	1.9	0.0	90.9	99.1
Ethyl acetate	141–78-6	11.2	10.5	82.7	89.6	1.2	0.0	0.3	0.0	4.6	0.0	83.9	89.6
Ethyl lactate	97–64-3	0.2	0.2	22.7	24.8	34.2	40.4	7.2	9.7	35.7	24.9	56.9	65.2
Ethyl caproate	123–66-0	11.3	6.4	85.7	93.6	1.1	0.0	0.2	0.0	1.6	0.0	86.8	93.7
Ethyl caprylate	106–32-1	9.0	7.5	90.4	92.5	0.6	0.0	0.0	0.0	0.0	0.0	91.0	92.5
Ethyl caprate	110–38-3	6.7	5.7	91.7	94.3	1.4	0.0	0.2	0.0	0.1	0.0	93.1	94.3
Isoamyl acetate	123–92-2	11.8	10.7	86.6	89.3	0.4	0.0	0.2	0.0	1.0	0.0	87.0	89.3
Ethyl butanoate	105–54-4	11.4	13.2	80.7	86.9	1.9	0.0	0.4	0.0	5.6	0.0	82.6	86.9
Hexyl acetate	142–92-7	9.8	6.2	90.2	93.8	0.0	0.0	0.0	0.0	0.0	0.0	90.2	93.8
Acetaldehyde	75–07-0	5.1	10.2	94.9	90.0	0.0	0.0	0.0	0.0	0.0	0.0	94.9	90.0
Furfural	98–01-1	0.9	0.5	44.6	43.4	54.5	38.3	0.0	6.5	0.0	11.2	99.1	81.7
1,1-Diethoxy-ethane	105–57-7	4.2	8.4	95.8	91.7	0.0	0.1	0.0	0.0	0.0	0.0	95.8	91.8
Acetic acid	64–19-7	0.3	0.1	10.8	6.3	8.8	9.7	4.0	3.4	76.2	80.5	19.6	16.0
Isobutanoic acid	79–31-2	0.0	0.2	24.7	16.1	39.6	26.5	10.3	8.0	25.4	49.2	64.3	42.6
Isovaleric acid	503–74-2	0.0	0.3	0.0	25.1	38.9	39.4	14.0	9.3	47.2	25.8	38.9	64.5
Caproic acid	142–62-1	0.1	0.0	22.6	11.6	49.0	58.1	11.8	13.4	16.5	16.8	71.6	69.7
Caprylic acid	124–07-2	0.3	0.2	30.2	36.0	54.7	58.3	9.8	3.9	5.1	1.6	84.9	94.2

flowmeter density and temperature measurement was reliable. Indeed, for the first eight comparisons, the maximum difference did not exceed 1%. However, it should be emphasised that the Coriolis flowmeter may be less accurate at low ethanol concentrations, as evidenced by the difference of 5.12% in the last comparison.

The ethanol concentration, total mass and ethanol mass were calculated from both offline and online data for each fraction of distillate, except for the heads and *petites-eaux*, which did not pass through the Coriolis flowmeter. Differences are presented in Table 4. For the heart fraction, distillate and ethanol masses were lower online than offline, while the ethanol mass fraction difference was the lowest (0.46%). Mass differences may be caused by an underestimated flow rate value. For the seconds, masses were also lower online than offline, but to a lesser extent. In contrast, online and offline masses of the tails were similar, while the difference in ethanol concentration was the highest (6.85%). Nonetheless, the similarity of these results suggests that the data recorded by the Coriolis flowmeter were globally coherent and could be used later to adjust the simulation.

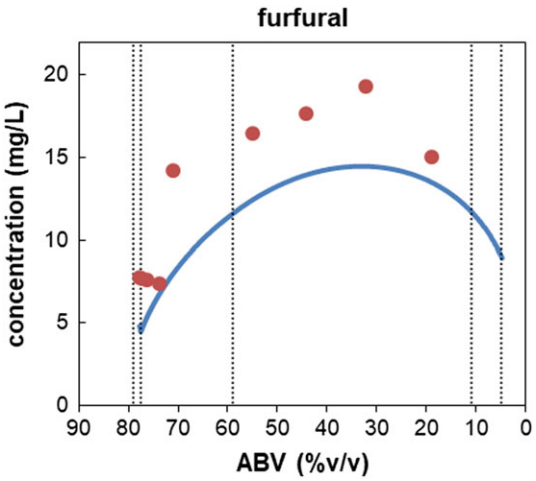

Figure 9. Experimental and simulated concentration profiles for furfural. [Colour figure can be viewed at wileyonlinelibrary.com]

Volatile compound mass balances

Among the 69 volatile compounds analysed in the low wine, only 45 (nine alcohols, one carbonyl compound, one furan, one acetal, 18 esters, three terpenes and 12 carboxylic acids) were above their quantification limits. The total mass balance of each compound was established by comparing the mass contained in the boiler (In) and the sum of masses in the distillate and residue fractions (Out). These ratios (Out/In) are presented in Table 5 with volatile compounds previously analysed by Cantagrel *(7)* indicated with a [a] (six alcohols, one carbonyl compound, one furan, one acetal, 16 esters and three carboxylic acids).

As observed previously by several authors *(9,23)*, the mass balance ratio for alcohols at high concentrations is close to 1.

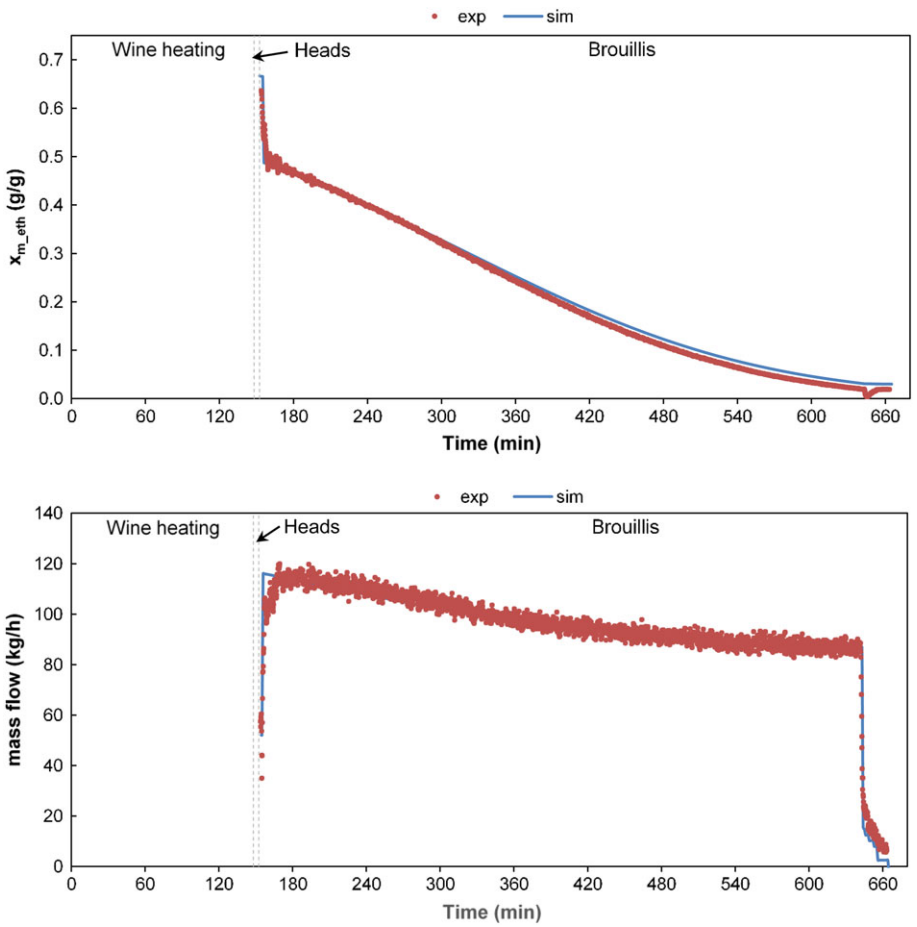

Figure 10. Experimental and simulated profiles during wine distillation in 2500 L still. [Colour figure can be viewed at wileyonlinelibrary.com]

However, for many volatile compounds present at low concentrations, outputs were often lower than inputs (Out/In <1). This may be due to analytical issues, volatilisation of the compound at the condensing coil output or chemical reactions. On the contrary, a ratio above 1 (Out/In >1) indicates either the formation of volatile compounds during distillation or analytical issues. Despite these differences, the 45 volatile compounds were considered in the rest of this study.

The experimental concentration profiles of volatile compounds during distillation

The concentrations of the 45 volatile compounds were plotted as a function of decreasing ABV of the distillate and classified according to Figure 2. In Table 6, this classification is compared with that proposed by Cantagrel *(7)*. Among the 45 volatile compounds, only 28 were quantified in both studies and 22 had a similar classification to that proposed *(7)*. In the report of Cantagrel, ethyl caprylate and ethyl caprate were classified as type 8, whereas in this study they were considered as type 1 (Table 6; Fig. 4a, 4b). However, type 1 and type 8 have similar profiles and this modification may be explained by a small change in the distillation process. In the past, yeast residues containing ethyl caprylate and ethyl caprate were introduced into the boiler just after the end of the heart distillation, while this residue is no longer distilled with the low wine but blended into the wine. Ethyl stearate, ethyl oleate and ethyl linoleate were classified as type 1 instead of type 7 (Fig. 4c, 4d, 4e), and 2-phenylethanol was classified as type 6 instead of type 2 (Fig. 4f). However, in each case, it should be emphasised that the shapes of both concentration profiles are comparable. Among the other compounds not analysed by Cantagrel *(7)*, linalool, myristic acid, palmitic acid and 2-phenylethyl caprylate are not considered as their concentration profiles were not correctly represented, which may reflect analytical issues.

These results are similar to the classification of volatile compounds into three groups (light, intermediate and heavy) proposed by Puentes *et al. (28)*, in the low ethanol concentrations in the liquid phase ($<30\%$ v/v). As shown in Table 7, the classifications of the 24 volatile compounds considered in both studies were consistent with each other: all of the type 1 and type 7 species were classified as light compounds, types 3 and 6 as intermediate compounds, and type 2 as heavy compounds.

Comparison of experimental and simulated data

In order to evaluate the capacity of the simulation tool to represent experimental online data collected by the Coriolis flowmeter accurately, experimental and simulated ethanol concentrations and mass flow data were plotted (Fig. 5). The alignment of both curves indicated that the simulated data were consistent with the experimental data. Therefore, it was concluded that the design of the batch distillation unit, together with the heating power and internal reflux levels, was properly configured in the software.

Subsequently, the simulation tool was used to present the concentration profiles of the volatile compounds during distillation, as well as their distribution in the distillate fractions. Among the 41

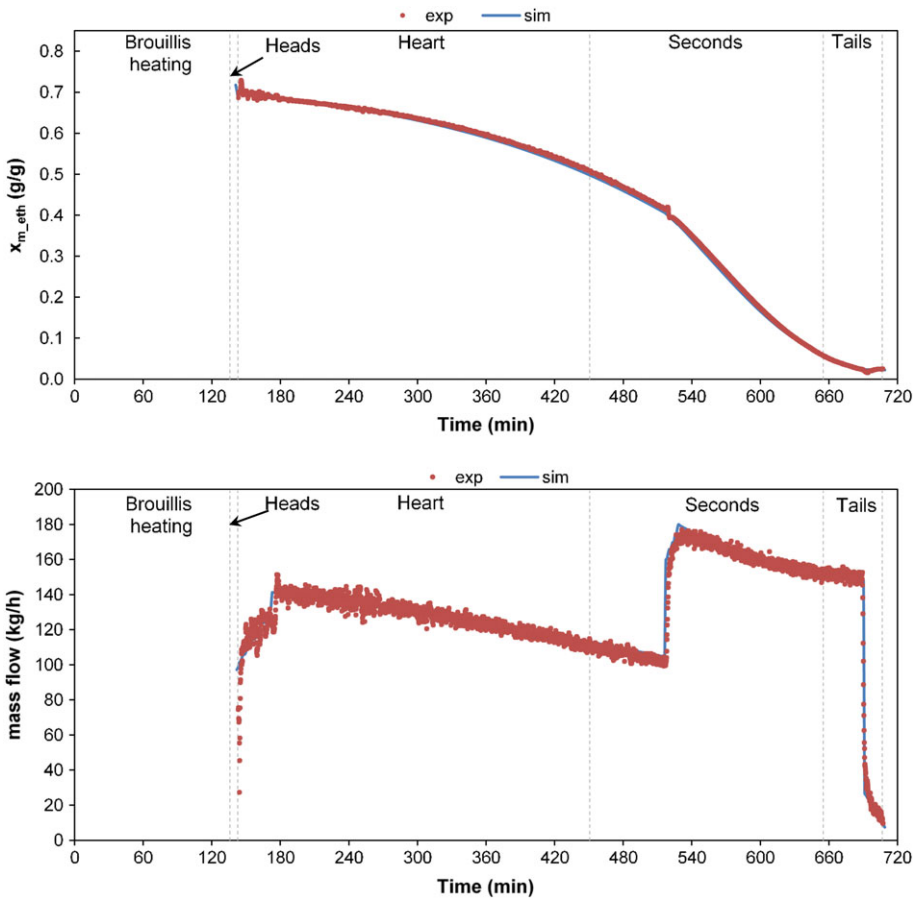

Figure 11. Experimental and simulated profiles during low wine distillation in 2500 L still. [Colour figure can be viewed at wileyonlinelibrary.com]

volatile compounds clearly identified by type (Table 6), 26 were available in the ProSim database and their NRTL coefficients were known. The consistency of simulated profiles with experimental data is presented in Table 8. The simulated curves for 18 volatile compounds were overlaid on experimental data. An example (isoamyl acetate) is shown in Figure 6a. For seven of these compounds, the shape of the curve was the same but the maximum concentration was different (e.g. ethyl lactate in Figure 6b) or the maximum was obtained at a different ABV value (e.g. 1-hexanol in Figure 7d). Finally, only one volatile compound (formic acid) showed inconsistencies between the simulated and experimental data.

The simulation data were the most consistent for alcohols present in the distillate at high concentration (2-methyl-1-propanol, 3-methyl-1-butanol) (Fig. 7a). Nevertheless, for 2-methyl-1-butanol, also present at high concentration, a shift in the maximum concentration value was observed between the simulated and experimental data (Fig. 7b). The simulated 2-phenylethanol concentration profile was the same shape as the experimental one (Fig. 7c), but the experimental concentration in the tails fraction was lower than the simulated result, while all the other values were higher. This underestimated value may be related to the experimental mass balance ratio of 0.6 (Table 5). Finally, 1-hexanol presented a similar shape but a maximum concentration at a different ABV value (Fig. 7d).

For compounds with maximum concentrations at different ABV in the experimental and simulated data, it would be interesting to measure new equilibrium data, particularly at low ABV (<30% v/v), and estimate new NRTL coefficient for compounds with different maximum concentrations but at the same ABV, this may reflect analytical errors. It must be emphasised that most methods produce accurate results for the heart fraction but are not always adapted to analysing solutions with low ethanol concentrations.

Carboxylic acids were also simulated without taking into account dimerisation using the ideal gas law. According to the concentration profiles reported in Figure 8, the introduction of an association model improved the simulation, especially for acetic acid (Fig 8a), a small molecule whose dimerised fraction in the vapour phase is high. For larger molecules, such as isovaleric acid, dimerisation becomes less important, which explains why the simulation with both models is similar (Fig 8b).

Values of experimental distribution of the volatile compounds in the various distillate fractions were compared with simulated data. In some cases, as the experimental mass balances did not give a ratio (Out/In) close to 1, the distribution was calculated using the total output mass. As shown in Table 9, the distribution data calculated by simulation was close to the experimental results for most volatile compounds. Moreover, experimental and simulated results for the heart and seconds fractions together (Ht + S) were closer. However, some differences were noted. The simulation predicted a higher concentration of 2-phenylethanol in the residue (47.1%) compared with the experimental data (33.7%). This overestimated concentration in the residue is in agreement with the simulated concentration profile during distillation (Fig. 7c). Similarly, the simulation predicted 6.5% furfural in the tails and 11.2% in the residue, whereas this compound was not detected in these experimental fractions. This may be due to the underestimation of the simulated values (Fig. 9), because the experimental mass balance was in agreement, with an (Out/In) quotient very close to 1 (0.96) (Table 5). Only two compounds, isobutanoic and isovaleric acids,

Table 10. Distribution of volatile compounds during the wine distillation in a 2500 L copper still

		Heads (%)		Low wine (%)		Residue (%)	
	CAS	Experimental	Simulated	Experimental	Simulated	Experimental	Simulated
Ethanol	64–17-5	1.3	1.4	98.2	96.6	0.5	2.1
Methanol	67–56-1	0.9	0.6	96.3	84.8	2.8	14.6
1-Propanol	71–23-8	1.7	1.3	98.0	98.0	0.3	0.7
1-Butanol	71–36-3	2.4	1.7	97.6	98.2	0.0	0.1
2-Methyl-1-propanol	78–83-1	3.5	2.2	96.5	97.7	0.1	0.0
2-Methyl-1-butanol	137–32-6	3.4	2.7	96.5	97.3	0.1	0.0
3-Methyl-1-butanol	123–51-3	2.7	2.2	97.2	97.8	0.1	0.0
1-Hexanol	111–27-3	2.5	1.8	97.5	98.2	0.0	0.0
(*Z*)-3-Hexenol	928–96-1	1.0	1.5	99.0	98.3	0.0	0.1
2-Phenylethanol	60–12-8	0.1	0.1	40.9	42.4	59.0	57.6
Ethyl acetate	141–78-6	15.2	9.8	84.7	90.2	0.1	0.0
Ethyl lactate	97–64-3	0.1	0.2	68.0	55.3	32.0	44.5
Ethyl caproate	123–66-0	47.4	6.1	52.6	93.9	0.0	0.0
Ethyl caprylate	106–32-1	51.9	17.1	48.1	82.9	0.0	0.0
Ethyl caprate	110–38-3	52.9	29.9	47.1	70.1	0.0	0.0
Acetaldehyde	75–07-0	3.6	10.6	89.0	89.4	7.4	0.0
2-Methylpropanal	78–84-2	0.4	15.9	99.6	84.1	0.0	0.0
Propanal	123–38-6	1.6	5.3	86.3	94.7	12.1	0.0
Butanal	123–72-8	3.1	10.7	82.0	89.3	14.9	0.0
3-Methylbutanal	590–86-3	5.4	15.6	93.6	84.4	0.9	0.0
Pentanal	110–62-3	4.1	9.9	95.9	90.1	0.0	0.0
Furfural	98–01-1	0.0	0.4	99.1	74.1	0.9	25.5
1.1-Diethoxyethane	105–57-7	3.3	4.2	81.2	95.8	15.5	0.0
Linalool	78–70-6	2.3	4.8	96.7	95.2	1.0	0.0

Table 11. Distribution of volatile compounds during the low wine distillation in a 2500 L copper still

	Heads (%)		Heart (%)		Seconds (%)		Tails (%)		Residue (%)		Heart + seconds (%)	
	Experimental	Simulated	Experimental	Simulated	Experimental	Simulated	Experimental	Simulated	Experimental	Simulated	Experimental	Simulated
Ethanol	1.4	1.4	73.0	72.8	24.7	24.4	0.7	0.6	0.1	0.8	97.7	97.2
Methanol	1.2	1.0	62.6	57.67	31.5	32.08	2.3	2.31	2.5	6.9	94.1	89.7
1-Propanol	1.4	1.5	80.9	78.7	17.3	19.6	0.1	0.2	0.2	0.1	98.3	98.2
1-Butanol	1.2	1.6	83.9	83.4	14.9	15.0	0.0	0.0	0.0	0.0	98.8	98.4
2-Methyl-1-propanol	2.1	2.1	91.5	89.8	6.4	8.1	0.0	0.0	0.0	0.0	97.9	97.9
2-Methyl-1-butanol	1.7	0.9	92.3	84.0	6.0	15.0	0.0	0.0	0.0	0.0	98.3	99.1
3-Methyl-1-butanol	1.4	1.6	90.5	87.0	8.1	11.4	0.0	0.0	0.0	0.0	98.6	98.4
1-Hexanol	0.9	0.9	90.8	78.5	8.3	20.5	0.0	0.0	0.0	0.0	99.1	99.1
(*Z*)-3-Hexenol	0.5	1.0	71.7	76.7	27.8	22.2	0.0	0.1	0.0	0.0	99.5	98.9
2-Phenylethanol	0.0	0.0	11.5	4.7	44.7	28.0	6.9	6.9	36.8	60.4	56.2	32.7
Ethyl acetate	9.8	9.7	89.4	90.3	0.7	0.0	0.0	0.0	0.1	0.0	90.1	90.3
Ethyl lactate	0.1	0.1	23.2	15.6	47.1	35.6	7.9	6.3	21.6	42.4	70.4	51.2
Ethyl caproate	11.6	5.9	88.4	94.0	0.0	0.1	0.0	0.0	0.0	0.0	88.4	94.1
Ethyl caprylate	8.0	7.7	88.4	92.3	3.4	0.0	0.2	0.0	0.0	0.0	91.8	92.3
Ethyl caprate	4.9	6.3	92.4	93.7	2.5	0.0	0.2	0.0	0.0	0.0	94.9	93.7
Acetaldehyde	5.8	8.9	71.2	91.1	3.6	0.0	0.3	0.0	19.2	0.0	74.8	91.1
2-Methylpropanal	16.6	12.5	83.4	87.5	0.0	0.0	0.0	0.0	0.0	0.0	83.4	87.5
Propanal	3.8	8.7	49.4	91.2	32.7	0.0	1.2	0.0	12.8	0.0	82.2	91.3
Butanal	5.9	12.8	57.1	87.2	25.7	0.0	0.8	0.0	10.4	0.0	82.9	87.2
3-Methylbutanal	14.2	12.7	85.3	87.2	0.3	0.0	0.0	0.0	0.2	0.0	85.6	87.3
Pentanal	5.4	10.8	57.4	89.2	22.4	0.0	0.8	0.0	14.0	0.0	79.8	89.2
Furfural	0.3	0.4	45.8	35.5	44.5	40.6	4.1	4.6	5.2	18.9	90.4	76.1
1,1-Diethoxyethane	3.9	7.1	70.7	92.6	2.2	0.2	0.4	0.0	22.8	0.0	72.9	92.9
Linalool	1.2	0.9	95.4	92.8	3.2	6.3	0.0	0.0	0.3	0.0	98.6	99.1

presented inconsistent distribution between experimental and simulated data. Their corresponding equilibrium data and chemical analyses require further study.

Assessment of the simulation tool on other experimental data

In order to assess the potential of the simulation tool to represent wine and low wine distillations in a standard size copper still (2500 L), experimental data from Awad *et al. (9)* were used as reference. The simulation module was configured as reported previously (three intermediate trays with 0.1 kg retention and 0.63 efficiency, a cooler with 0.1 kg retention, and a boiler with 0.9 efficiency). The heating power, reflux ratio and duration of each step were chosen according to the control parameters. Experimental and simulated ethanol concentrations and distillate mass flows during wine distillation are illustrated in Figure 10. Figure 11 shows the same data for the low wine distillation. As in the previous comparison, simulated data were in good agreement with experimental results for both ABV and mass flow of the distillate. Thus, simulation proved to be a suitable tool for studying the behaviour of volatile compounds during traditional distillation.

The experimental distribution of 23 volatile compounds in the distillate fractions were compared with simulated data for wine (Table 10) and low wine distillation (Table 11). Unlike the previous study in the 600 L copper still, carboxylic acids were not quantified. Most volatile compounds were well represented by simulation for both distillations. It should be noted that the simulated distribution of 2-phenylethanol in wine distillation was close to the experimental results (Table 10), but the proportion of 2-phenylethanol in the residue (60.4%) from the low wine distillation predicted by simulation (Table 11) was higher than the experimental value (36.8%). A similar difference had already been observed for the low wine distillation in the 600 L alembic still, where the mass balance (Out/In) was 0.6. Despite the fact that acetaldehyde and 1,1-diethoxyethane were classified as light volatile compounds with type 1 concentration profiles, it is interesting to note that they were quantified in the residue of both wine and low wine distillations (Tables 10, 11). These experimental results were probably due to analytical errors, owing to the very low ethanol content of the residue (e.g. incorrect assignment of overlapping chromatographic peaks, slight delays in retention times due to matrix effects, etc.). This argument is supported by the study using the 600 L boiler, where the concentration of these compounds in the residue was zero, as predicted by the simulation. The same explanation of analytical errors may apply to the presence of propanal and butanal in the residue. For the wine distillation, even if ethyl caproate, ethyl caprylate and ethyl caprate were classified as type 1 (Table 6), their high concentration in the head fraction of the wine distillation (Table 10) was unexpected and may also be due to analytical errors.

Conclusion

This study was conducted in 600 L (laboratory scale) and 2500 L (industrial scale) copper stills, both equipped with a Coriolis flowmeter on the distillate line after the alcoholmeter. Among the 69 volatile compounds initially analysed, 45 were quantified in the samples of the laboratory experiment. The concentration profiles as a function of decreasing distillate ABV were analysed to confirm and complete the classification proposed by Cantagrel *(7)*. Simulations were performed with ProSim® BatchColumn software. Twenty-six species were included in the simulation, considering the interaction parameters of the NRTL model, estimated from equilibrium data at high dilution *(26)*. Good correlation was observed between experimental and simulated data in terms of ABV, mass flow, concentration profiles, concentration of the volatile compounds and distribution in the various distillate fractions. This consistency also validated the NRTL coefficients determined by Puentes *et al. (26)*. However, for some volatile compounds, it would be useful to verify their equilibrium data at low ethanol concentrations to improve the consistency of simulated data with experimental findings. From an experimental point of view, the recorded data from a Coriolis flowmeter placed in the distillate flow (i.e. volume flow, temperature and density of the distillate over time) were sufficient to simulate the distillation process. Indeed, from the Coriolis flowmeter data, it was possible to calculate the mass flow and ethanol concentration over time and, consequently, to adjust the simulation parameters, such as heating power and internal reflux level.

In the future, it would be interesting to take into account the recycling of distillate fractions, as most distilleries blend the heads and tails into the wine and the seconds into the low wine. An experimental sampling and measurement programme, following successive distillations, could be designed with the aim of determining the heart composition and compare it with the base wine composition. Elucidating the behaviour of volatile compounds throughout the whole Charentais distillation process would highlight the main differences between batch distillations and continuous distillation in multi-stage columns, used for Armagnac and Calvados production. This knowledge would also be useful in the longer term for developing optimisation strategies to control distillate composition, which is intimately linked to quality, as well as to reduce energy consumption.

Acknowledgements

The authors would like to thank ProSim, for a free licence of BatchColumn and technical advice during this study. They are also grateful to the Union Nationale du Groupement des Distillateurs d'Alcool for analytical support.

References

1. Official Journal of the European Regulation (2008) Regulation (EC) no.110/2008 of the European parliament and of the council of 15 January 2008 on the definition, description, labelling and the protection of geographical indications of spirit drinks and repealing Council Regulation no. 1576/89.
2. Nykänen, L., and Suomalainen, H. (1983) *Aroma of beer, wine and distilled alcoholic beverages, handbook of aroma research*, 1st ed., Springer, Dordrecht.
3. Decloux, M., and Joulia, X. (2009) Distillation of AOC French spirits: Cognac, Armagnac, Calvados and Martinique agricultural rum, in *The Alcohol Textbook*, (Ingledew, W. M., and Kelsall, D. R., and Austin, G. D., and Kluhpies, C. Eds.), pp. 491–506, Nottingham University Press, Nottingham.
4. Ledauphin, J., Milbeau, C. L. E., Barillier, D., and Hennequin, D. (2010) Differences in the volatile compositions of french labeled brandies (Armagnac, Calvados, Cognac, and Mirabelle) using GC-MS and PLS-DA, *J. Agric. Food Chem. 58*, 7782–7793. https://doi.org/10.1021/jf9045667.
5. Gaiser, M., Lim, A. W., Roberts, N. A., Faraday, D. B. F., Schulz, R. A., and Gorb, R. (2002) Computer simulation of a continuous whisky still, *J. Food Eng. 51*, 27–31. https://doi.org/10.1016/S0260-8774(01)00033-4.
6. Ferrari, G., Lablanquie, O., Cantagrel, R., Ledauphin, J., Payot, T., Fournier, N., and Guichard, E. (2004) Determination of key odorant compounds in freshly distilled Cognac using GC-O, GC-MS, and sensory evaluation, *J. Agric. Food Chem. 52*, 5670–5076. https://doi.org/10.1021/jf049512d.

7. Cantagrel, R. (1989) A scientific approach to quality control for Cognac spirits, in *Distilled Beverage Flavour, Recent Developments*, (Piggott, J. R., and Paterson, A. Eds.), pp. 117–132, Ellis Horwood/VCH, Chichester.
8. Cantagrel, R., and Galy, B. (2003) From vine to Cognac, in *Fermented Beverage Production*, (Lea, A. G. H., and Piggott, J. R. Eds.) 2nd ed., pp. 195–212, Kluwer Academic/Plenum, New York.
9. Awad, P., Athès, V., Esteban-Decloux, M., Ferrari, G., Snakkers, G., Raguenaud, P., and Giampaoli, P. (2017) Evolution of volatile compounds during the distillation of Cognac spirit, *J. Agric. Food Chem. 65*, 7736–7748. https://doi.org/10.1021/acs.jafc.7b02406.
10. BO AGRI (2015) Cahier Des Charges de L'appellation D'origine Contrôlée 'Cognac' Ou 'Eau-de-Vie de Cognac' Ou 'Eau-de-Vie Des Charentes' Homologué Par Le Décret N° 2015–10 Du 7 Janvier 2015 Relatif à L'appellation D'origine Contrôlée 'Cognac' Ou 'Eau-de-Vie de Cognac' Ou 'Eau-de-Vie Des Charentes'. Bulletin officiel du ministère chargé de l'agriculture. https://info.agriculture.gouv.fr/gedei/site/bo-agri/document_administratif-3c5294fb-47c8-40b1-8564-84dcb74140e9.
11. Lukić, I., Tomas, S., Miličević, B., Radeka, S., and Peršurić, D. (2011) Behaviour of volatile compounds during traditional alembic distillation of fermented Muscat Blanc and Muškat Ruža Porečki grape marcs, *J. Inst. Brew. 117*, 440–450. https://doi.org/10.1002/j.2050-0416.2011.tb00491.x.
12. Spaho, N., Dürr, P., Grba, S., Velagić-Habul, E., and Blesić, M. (2013) Effects of distillation cut on the distribution of higher alcohols and esters in brandy produced from three plum varieties, *J. Inst. Brew. 119*, 48–56. https://doi.org/10.1002/jib.62.
13. Silva, F. A., Vendruscolo, F., Carvalho, W. R., Soares Júnior, M. S., Pinheiro, M. V. M., and Caliari, M. (2013) Influence of the number of distillations on the composition of organic sugarcane spirit, *J. Inst. Brew. 119*, 133–138. https://doi.org/10.1002/jib.78.
14. Balcerek, M., Pielech-Przybylska, K., Patelski, P., Dziekońska-Kubczak, U., and Strąk, E. (2017) The effect of distillation conditions and alcohol content in 'heart' fractions on the concentration of aroma volatiles and undesirable compounds in plum brandies, *J. Inst. Brew. 123*, 452–463. https://doi.org/10.1002/jib.441.
15. Batista, F. R. M., and Meirelles, A. J. A. (2011) Computer simulation applied to studying continuous spirit distillation and product quality control, *Food Control 22*, 1592–1603. https://doi.org/10.1016/j.foodcont.2011.03.015.
16. Batista, F. R. M., Follegatti-Romero, L. A., Bessa, L. C. B. A., and Meirelles, A. J. A. (2012) Computational simulation applied to the investigation of industrial plants for bioethanol distillation, *Comp. Chem. Eng. 46*, 1–16. https://doi.org/10.1016/j.compchemeng.2012.06.004.
17. Valderrama, J. O., Faúndez, C. A., and Toselli, L. A. (2012) Advances on modeling and simulation of alcoholic distillation. Part 1: Thermodynamic modeling, *Food Bioprod. Process. 90*, 819–831. https://doi.org/10.1016/j.fbp.2012.04.004.
18. Valderrama, J. O., Faúndez, C. A., and Toselli, L. A. (2012) Advances on modeling and simulation of alcoholic distillation. Part 2: Process simulation, *Food Bioprod. Process. 90*, 832–840. https://doi.org/10.1016/j.fbp.2012.04.003.
19. Esteban-Decloux, M., Deterre, S., Kadir, S., Giampaoli, P., Albet, J., Joulia, X., and Baudouin, O. (2014) Two industrial examples of coupling experiments and simulations for increasing quality and yield of distilled beverages, *Food Bioprod. Process. 92*, 343–354. https://doi.org/10.1016/j.fbp.2013.10.001.
20. Osorio, D., Pérez-Correa, J. R., Belancic, A., and Agosin, E. (2004) Rigorous dynamic modeling and simulation of wine distillations, *Food Control 15*, 515–521. https://doi.org/10.1016/j.foodcont.2003.08.003.
21. Osorio, D., Pérez-Correa, J. R., Biegler, L. T., and Agosin, E. (2005) Wine distillates: Practical operating recipe formulation for stills, *J. Agric. Food Chem. 53*, 6326–6331. https://doi.org/10.1021/jf047788f.
22. Scanavini, H. F. A., Ceriani, R., Cassini, C. E. B., Souza, E. L. S., Maugeri Filho, F., and Meirelles, A. J. A. (2010) Cachaça production in a lab-scale alembic: Modelling and computational simulation, *J. Food Process Eng. 33*, 226–252. https://doi.org/10.1111/j.1745-4530.2008.00352.x.
23. Sacher, J., Garcia-Llobodanin, L., Lopez, F., Segura, H., and Perez-Correa, J. R. (2013) Dynamic modeling and simulation of an alembic pear wine distillation, *Food Bioprod. Process. 91*, 447–456. https://doi.org/10.1016/j.fbp.2013.04.001.
24. Gmehling, J., Li, J., and Schiller, M. A. (1993) Modified UNIFAC model. 2. Present parameter matrix and results for different thermodynamic properties, *Ind. Eng. Chem. Res. 32*, 178–193. https://doi.org/10.1021/ie00013a024.
25. Athès, V., Paricaud, P., Ellaite, M., Souchon, I., and Fürst, W. (2008) Vapour–liquid equilibria of aroma compounds in hydroalcoholic solutions: Measurements with a recirculation method and modelling with the NRTL and COSMO-SAC approaches, *Fluid Phase Equilib. 265*, 139–154. https://doi.org/10.1016/j.fluid.2008.01.012.
26. Puentes, C., Joulia, X., Athès, V., and Esteban-Decloux, M. (2018) Review and thermodynamic modeling with NRTL model of vapor-liquid equilibria (VLE) of aroma compounds highly diluted in ethanol-water mixtures at 101.3 kPa, *Ind. Eng. Chem. Res. 57*, 3443–3470. https://doi.org/10.1021/acs.iecr.7b03857.
27. Renon, H., and Prausnitz, J. M. (1968) Local compositions in thermodynamic excess functions for liquid mixtures, *AICHE J. 14*, 135–144. https://doi.org/10.1002/aic.690140124.
28. Puentes, C., Joulia, X., Vidal, J. P., and Esteban-Decloux, M. (2018) Simulation of spirits distillation for a better understanding of volatile aroma compounds behavior: Application to Armagnac production, *Food Bioprod. Process. 112*, 31–62. https://doi.org/10.1016/j.fbp.2018.08.010.
29. International Organization of Legal Metrology (1975). International Alcoholometric Tables, OIML R 22. Available from: https://www.itecref.com/pdf/OIML_Alcoholometric_Tables.pdf. Accessed 10 july 2017.
30. Detcheberry, M., Destrac, P., Massebeuf, S., Baudouin, O., Gerbaud, V., Condoret, J. S., and Meyer, X. M. (2016) Thermodynamic modeling of the condensable fraction of a gaseous effluent from lignocellulosic biomass torrefaction, *Fluid Phase Equilib. 409*, 242–255. https://doi.org/10.1016/j.fluid.2015.09.025.